A Digital CRISPR-based Method for the Rapid Detection and Absolute Quantification of Viral Nucleic Acids

Xiaolin Wu[1], Cheryl Chan[1], Yie Hou Lee[1], Stacy L. Springs[1,2], Timothy K. Lu[1,3,4,5,6,7,8*], Hanry Yu [1,9,10,11*]

[1]Singapore-MIT Alliance for Research and Technology, Critical Analytics for Manufacturing of Personalized Medicine Interdisciplinary Research Group, Singapore 138602, Singapore

[2] Center for Biomedical Innovation, Massachusetts Institute of Technology, Cambridge, MA, USA.

[3]Synthetic Biology Center, Massachusetts Institute of Technology (MIT), Cambridge, MA 02139, USA

[4]Synthetic Biology Group, Research Laboratory of Electronics, Massachusetts Institute of Technology (MIT), Cambridge, MA 02139, USA

[5]Broad Institute of MIT and Harvard, Cambridge, MA 02142, USA

[6]Department of Electrical Engineering and Computer Science, Massachusetts Institute of Technology (MIT), Cambridge, MA 02142, USA

[7]Harvard-MIT Division of Health Sciences and Technology, Cambridge, MA 02139, USA

[8]Department of Biological Engineering, Massachusetts Institute of Technology (MIT), Cambridge, MA 02142, USA

[9]Institute of Bioengineering and Nanotechnology, A*STAR, The Nanos, #04-01, 31 Biopolis Way, Singapore 138669, Singapore

[10]Mechanobiology Institute, National University of Singapore, T-Lab, 5A Engineering Drive 1, Singapore 117411, Singapore

[11]Department of Physiology, National University of Singapore, MD9 #03-03, 2 Medical Drive, Singapore 117597, Singapore

* Correspondence should be addressed to Timothy K. Lu (timlu@mit.edu) and Hanry Yu (phsyuh@nus.edu.sg).

Abstract

Since the outbreak of SARS-CoV-2, quantitative real-time PCR and CRISPR-based methods have been increasingly used for virus detection because of their speed (1 hour) and sensitivity. However, these methods do not allow for the absolute quantification of virus particles, which could reduce the inter-lab variability and accelerate the virus research. Although there is a digital PCR-based method that has been used for absolute virus quantification, its reaction time (4 hours) is too long for widespread application. Here, we report a rapid digital CRISPR method developed for the absolute quantification of SARS-CoV-2 DNA and Epstein–Barr virus DNA in human samples that yields results within 1 hour. We validated this method using synthetic SARS-CoV-2 DNA and

Epstein–Barr viral DNA and compared results with those obtained with digital PCR. Digital CRISPR allows absolute quantification of DNA with a dynamic range from 0.6 to 2027 copies/µL (R^2 value > 0.98), without cross reactivity on similar virus and human background DNA. Thus, our digital CRISPR can accurately detect and quantify nucleic acid in 1h without thermal cycling, which provides a 4-fold faster alternative to digital PCR-based virus detection.

Keywords:

CRISPR, Molecular diagnosis, Absolute Quantification, SARS-CoV-2, virus detection

Introduction

COVID-19 is caused by severe acute respiratory syndrome coronavirus 2 (SARS-CoV-2) [1]. Methods to detect virus, as well as to quantify viral load, are needed for diagnostics, therapeutics, and vaccines to combat the worldwide spread of this infectious disease. The reverse transcription-polymerase chain reaction (RT-qPCR) is considered a gold standard for COVID-19 diagnosis. However, quantification via RT-qPCR relies on the use of external standards or references, and the results can be variable, with a 20–30% variability reported even within trained laboratories [2-4]. Thus, an absolute quantification method with improved precision and accuracy is vital for virus research [5-7].

Digital PCR is increasingly being used as a highly accurate and sensitive method for the absolute quantification of nucleic acids [2, 8-10]. In a digital PCR reaction, the PCR mixture is separated into thousands of individual reactions, resulting in the amplification of either zero or one of the nucleic acid target molecules present in each partition. After independent PCR amplification and endpoint fluorescence detection of each partition, the copy number of the sample is determined based on the proportion of positive partitions. Since the PCR reaction in each partition proceeds independently, absolute quantification by digital PCR is more precise than RT-qPCR and more tolerant of inhibitors; furthermore, digital PCR overcomes poor amplification efficiency [2].

The sensitivity and precision of digital PCR-based viral detection have been demonstrated in quantitative detection and viral load analysis of SARS-CoV-2-infected patient samples with a limit of detection (LOD) at ~2 copies/reaction with reduced inter-lab variability and fewer false negatives and fewer false positives compared with RT-PCR [7, 11-16]. Absolute quantification of the virus will lead to less variability between different labs. In addition to its application in viral diagnostics, digital PCR has also been applied to other areas of virus research, including the study of the aerodynamic transmission of SARS-CoV-2 [6] and in quantifying residual SARS-CoV-2 load in pulmonary tissues of a patient who tested virus-negative by the nasopharyngeal swab-qPCR test [5]. The main

drawback of digital PCR, however, is the relatively long reaction time (~4 hours) needed as a result of the 1-2°C/s ramp up/down rate for efficient inter-partition heat transfer during thermal cycling, compared to that of qPCR, which requires 1 hour. Reducing the reaction time of digital PCR is therefore crucial in enabling the adoption of the technology for rapid virus detection in hospitals and clinics[17].

Isothermal amplification methods, which amplify the nucleic acid target molecule at a constant temperature and thereby reduce the reaction time, have also been used for viral detection. These include methods that employ recombinase polymerase amplification (RPA) or loop-mediated isothermal amplification (LAMP) [18-23]. More recently, innovative diagnostic methods using RNA-guided CRISPR/Cas system have been developed to detect nucleic acids. In the RNA-guided CRISPR/Cas system, Cas effectors such as Cas12a, Cas12b and Cas13a are exploited for their collateral cleavage activity, which refers to the degradation of other nonspecific DNA/RNA oligos such as fluorescently-tagged reporter oligos, once the Cas protein finds and cleaves a specific DNA/RNA target [24, 25]. By combining RPA- or LAMP-mediated isothermal amplification of the target molecule with the CRISPR/Cas biosensing system, methods such as SHERLOCK and DETECTR have detected dengue virus and human papillomavirus, as well as SARS-CoV-2, in clinical samples [26-32]. However, as CRISPR-based methods are not quantitative and require multiple manipulations between the amplification and detection steps, there remains a need for a quantitative, rapid, and robust viral detection method.

Here, we report the development of a digital CRISPR method for the rapid, sensitive, and specific detection of viral nucleic acids at a constant temperature. This method combines the advantages of quantitative digital PCR, rapid isothermal amplification, and specific CRISPR detection into a one-pot reaction system that partitions the individual reactions into 10,000 compartments on a commercial high-density chip. In this study, we demonstrate an optimized digital CRISPR method that allows for absolute quantification of viral nucleic acids at a constant temperature in one hour. We validated this method using DNA containing the N (nucleoprotein) gene of SARS-CoV-2 and showed a linear signal-to-input response of R^2 value > 0.99. We compared our digital CRISPR detection system against the traditional digital PCR method and show that the digital CRISPR system (1h vs 4h) was faster and had sensitivity and accuracy comparable to that of traditional digital PCR. Also, this method is highly specific and do not have cross activity on other similar coronavirus. Furthermore, the absolute quantification results of this method are not influenced by 4000 copies of human background DNA. We also used digital CRISPR in the absolute quantification of Epstein–Barr virus from human B cells (R^2 value > 0.98). Our rapid and sensitive digital CRISPR method allows for the accurate detection and absolute quantification of viral nucleic acids.

Results

Design of digital CRISPR method

Commercial chips for sample partitioning and matched fluorescence reader for endpoint detection were used in digital CRISPR [33]. In this system, each CRISPR-based reaction mix is sub-divided into 10,000 partitions on the chip, resulting in an average partition volume of 1.336 nL. We first optimized the bulk CRISPR reaction to achieve a one-copy-per-1.336 nL partition detection sensitivity on the chip. This is equivalent to femtomolar detection sensitivity in a bulk reaction. We selected the Cas12a homolog from *Lachnospiraceae bacterium* ND2006 (LbCas12a) as it showed the highest signal-to-noise ratio relative to other Cas12a homologs from a previous study[27]. To test if the digital CRISPR method could detect viral DNA with femtomolar sensitivity without pre-amplification, serially-diluted dsDNA (double stranded DNA) was incubated with LbCas12a together with its CRISPR RNA (crRNA) and a reporter (quenched fluorescent DNA). The sensitivity of detection using the CRISPR-based method without pre-amplification in a bulk reaction was found to be 10 pM (Figure. S1), which did not meet the femtomolar sensitivity requirement of digital CRISPR.

To increase the sensitivity of detection of the CRISPR-based method, an isothermal amplification step was used. RPA was chosen for the isothermal amplification step because its reaction temperature (25°C to 42°C) is compatible with that of Cas12a (25°C to 48°C). This allowed for a one-step RPA-digital CRISPR absolute quantification method that eliminates multiple manipulations inherent in two-step CRISPR-based detection methods such as SHERLOCK and DETECTR [24, 25]. To avoid Cas12a-mediated cleavage of the target molecule before amplification, we designed the crRNA to target single-stranded DNA (ssDNA) that is generated only after amplification of the target molecule (Figure 1B) [32]. Another advantage of this method is the ease of designing ssDNA-targeting crRNA over traditional dsDNA-targeting crRNA, because the nuclease activity of Cas12a on ssDNA has been reported to be independent of the presence of protospacer adjacent motif (PAM) [34].

The digital CRISPR method developed in this study is illustrated in Figure 1A. Extracted DNA samples are loaded onto on the chip by capillary action, and the reaction is partitioned into 10,000 compartments, resulting in zero or one target molecule in each compartment. To prevent spontaneous target amplification by RPA at room temperature [35], the RPA-CRISPR reaction was prepared without the addition of Mg^{2+}, which is required for the polymerase activity. All reactions were prepared on ice and samples were loaded within one minute to prevent premature target amplification. The partitioned reactions were incubated in isothermal water baths, heat blocks, or warm rooms. In each compartment containing the target molecule (Figure 1B), RPA initiates from one DNA strand

and subsequently exposes the crRNA-targeted ssDNA region on the other strand. As the amplification proceeds, Cas12a cleaves the positive ssDNA strand, triggering its collateral cleavage activity, which in turn cleaves the proximal quenched fluorescent probe (ssDNA-FQ reporter) to generate a fluorescence signal. At the same time, ongoing amplification of the other DNA strand exponentially amplifies the target DNA, triggering more Cas12a activation and increasing the fluorescence readout. The proportion of positive-to-negative compartments is analyzed based on the endpoint fluorescence measurement, and the copy number of the target nucleic acid is calculated based on the Poisson distribution, allowing for absolute quantification of the sample (Figure 1A). Concurrent detection of compartments in each tube by the Clarity™ Reader shortens detection time to within minutes.

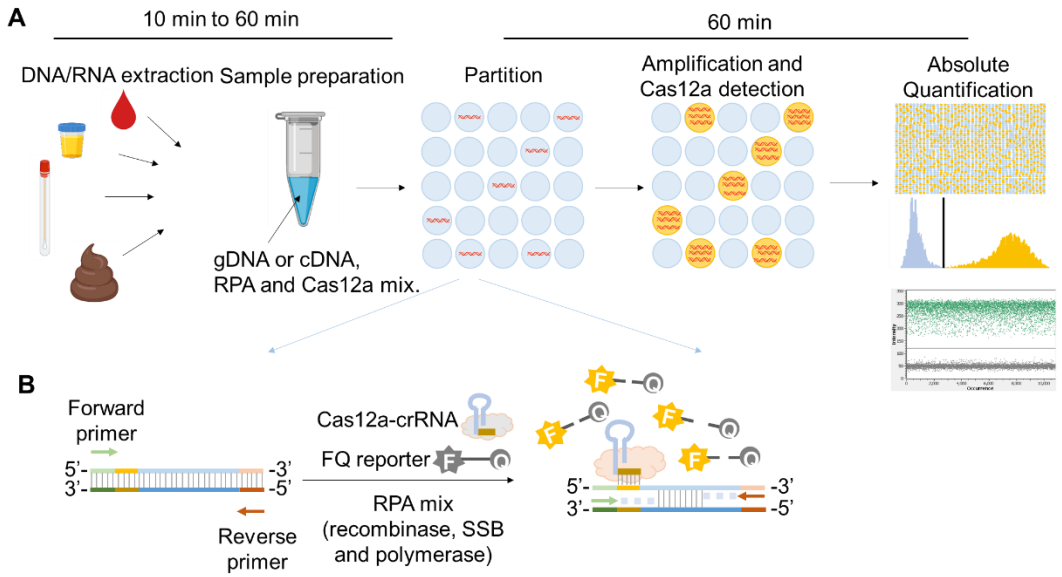

Figure 1. Schematic illustration of digital CRISPR method. A. The workflow of sample partitioning and digital CRISPR on a chip for absolute quantification of nucleic acid targets. Generally, after the DNA/RNA extraction step, different kind of clinical samples can be used for detection and quantification of various targets. The sample mixture containing DNA/cDNA, RPA reagents, and Cas12a-crRNA-FQ probes is distributed randomly into thousands of partitions. In each partition, the DNA is amplified by RPA and detected by Cas12a-crRNA, resulting in a fluorescent signal in the partition. Based on the proportion of positive partitions and on Poisson distribution, the absolute copy number of the nucleic acid target is quantified. **B.** Illustration of RPA-Cas12a reaction in each positive partition. In each partition containing the target nucleic acid, the primers bind to the target nucleic acid and initiate amplification with the aid of recombinase and DNA polymerase. Because of the strand displacement of DNA polymerase, the exposed crRNA-targeted ssDNA sites are bound by Cas12a-crRNA complexes. Cas12a is then activated and cleaves the nearby FQ reporters to produce a fluorescence readout.

Digital CRISPR method optimization

To validate and optimize the digital CRISPR method, G-block DNA or plasmids containing the SARS-CoV-2 N (nucleoprotein) gene region were used and primers and crRNAs specific for the SARS-CoV-2 N gene were designed accordingly based on previous studies [32]. The target regions overlap with those of the China CDC assay (N gene region) with some modification to meet the primer and crRNA design (Table S1). To optimize the Cas12a-mediated reaction, a bulk reaction using 0.1 nM and 1 nM dsDNA as a target was performed with a range of Cas12a/crRNA concentrations. We found that in the presence of a constant amount of target DNA and probe, comparable fluorescence signal intensities were detected between 50 nM to 250 nM Cas12a-crRNA concentrations, suggesting that changing the Cas12a/crRNA concentration did not influence the reaction (Figure S2).

Since the quenched fluorescent probe is another key component that influences the reaction, we optimized the FQ assay by incubating increasing amounts of FQ probes with constant concentrations of Cas12a-crRNA and target DNA. As expected, CRISPR-mediated fluorescence signal intensities increased with increasing amounts of FQ probes (from 250 nM to 5 μM), although higher probe concentrations also resulted in higher background noise (Figure 2A, 2B). At FQ probe concentrations above 5 μM, the signal-to-noise ratio could not be further enhanced (Figure 2B). To ensure that the fluorescence signal generated on the partitioned chip was within the reader's detection range, different FQ probe concentrations were tested in independent digital CRISPR reactions in the presence of the target DNA and the fluorescence measured on the digital PCR fluorescence reader. We found that in the presence of the same target DNA, the proportions of positive partitions were comparable regardless of the FQ probe concentration used (Figure 2D). However, only the background noise and positive signals generated in the reaction with 500 nM FQ probe concentration were within the reader's detection range, while the reactions containing 1000 nM FQ probe concentration yielded higher background noises, which are difficult to separate from positive signals (Figure 2C). We therefore used 500 nM FQ probe concentrations to achieve high signal-to-noise ratios for subsequent experiments.

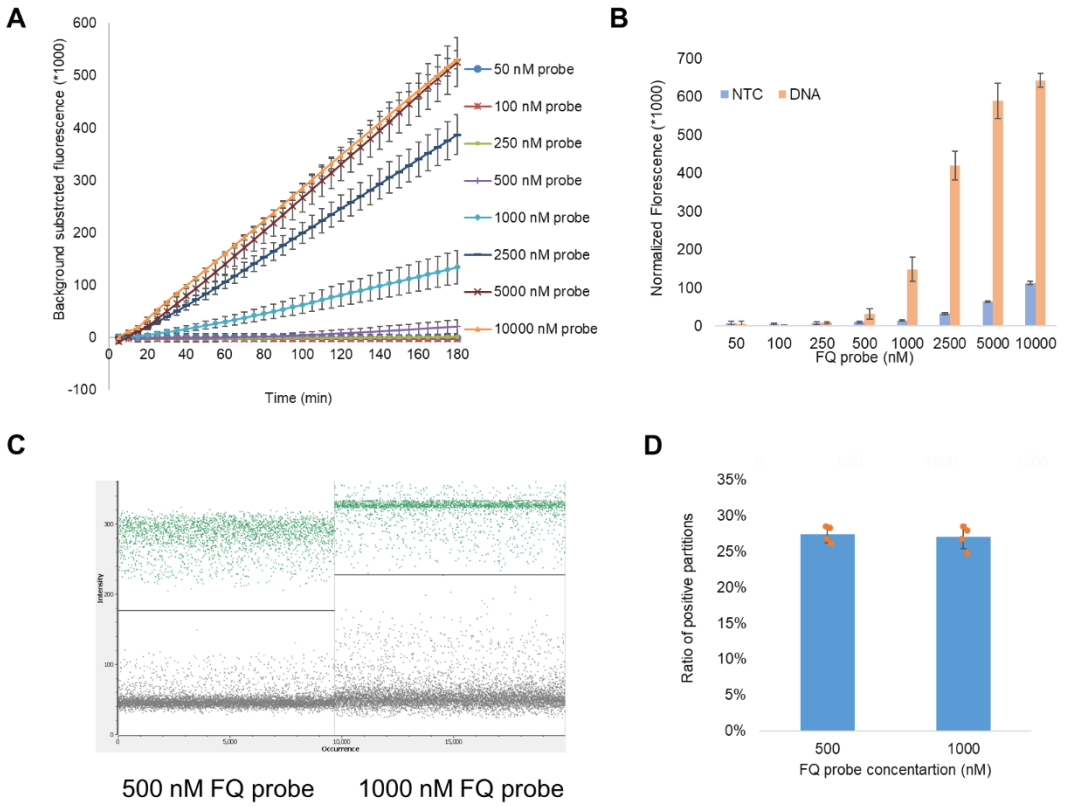

Figure 2. Optimization of FQ probe concentration in digital CRISPR method. A, B. Cas12a reaction in bulk reactions with different FQ probe concentrations in the presence or absence of a constant concentration (0.1 nM) of target DNA. **A.** Time course reaction of Cas12a with FQ probes at concentrations ranging from 50 nM to 10,000 nM. X-axis indicates the reaction time; y-axis indicates the background-subtracted fluorescence signal. **B.** Fluorescence signal of DNA and non-template control obtained with FQ probes at concentrations ranging from 50 nM to 10,000 nM. **C, D.** Digital CRISPR reaction with the same concentrations of target DNA but different probe concentrations. **C.** Fluorescence intensity of the negative partitions (background noise) and positive partitions (positive signals) on the chip obtained with FQ probes at concentrations of 500 or 1000 nM. **D.** Histogram showing ratios of positive partitions on the chip with FQ probes, at concentrations of 500 or 1000 nM, in the presence of target DNA (4 replicates for each FQ probe concentration).

An additional optimization step involved developing a one-pot reaction that combines the RPA and Cas12a reactions. We performed the bulk reaction at 25°C, 37°C and 42°C, which are temperatures within the reaction temperature ranges of RPA (25°C to 42°C) and Cas12a (25°C to 48°C). First, we tested the reaction using serial dilutions of plasmid DNA at 25°C and 42°C. The reaction proceeded at both of these reaction temperatures, with a limit of detection of about 9.4 copies/µL. However, at 25°C, the reaction proceeded significantly

more slowly with lower positive signals and a higher background than the reaction performed at a 42°C (Figure. S3). Next, we assessed the effect of different temperatures (25°C, 37°C and 42°C) on reactions containing a constant amount of plasmid DNA (37.5 copies/µL). We found that higher temperatures accelerated the reaction (Figure S3C). Taken together, our results suggest that 42°C is the optimal temperature for the RPA-Cas12a reaction.

We next investigated whether the reaction time affected the precision of digital CRISPR on plasmid DNA detection at 42°C. As shown in Figure 3A, the reaction proceeded quickly with some fluorescence signal detected in several compartments at 20 min, but with a low signal-to-noise ratio at this time point. As the reaction proceeded, two distinct peaks indicating the negative (left) and positive (right) partitions were detected at 40 min (Figure 3A). Analysis of the ratio of positive partitions on the chip at the different time points revealed that the number of positive partitions reached a plateau after 60 min in all four replicates, suggesting that 60 min was the earliest end-point measurement (Figure 3B). All subsequent experiments were therefore performed for 60 minutes.

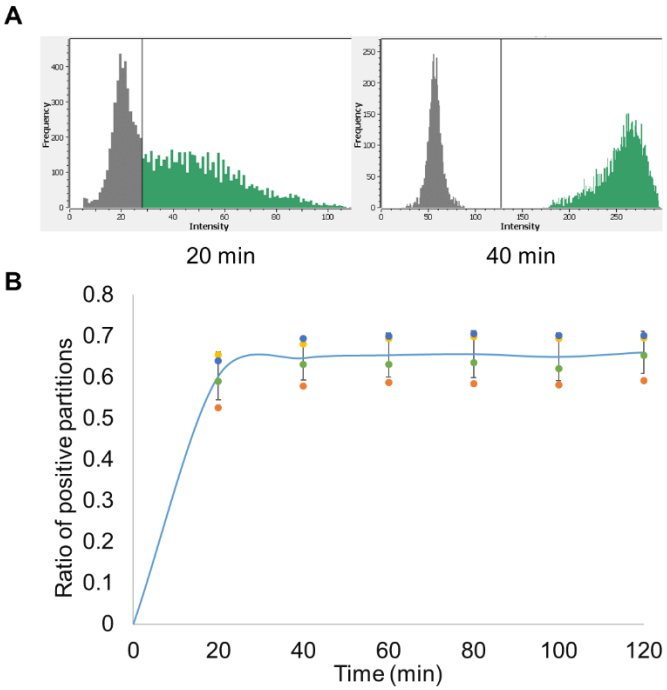

Figure 3. Time course reaction of digital CRISPR. A. Fluorescence intensity of the partitions on the chip at two time points. The x-axis represents fluorescence intensity while the y-axis represents the frequency of the partitions. The left peak (low fluorescence level; dark grey) on the fluorescence intensity histogram represents the negative partitions while the right peak (high fluorescence level; green) indicates the positive partitions. As the CRISPR reaction proceeds, the fluorescence levels of the positive partitions increase

and the right peak shifts further to the right. **B.** The proportion of positive partitions at different time points of digital CRISPR. Each DNA replicate is represented by a data point with a unique color. Starting at about 60 minutes, the fluorescence signal plateaus and the ratio of positive partitions reaches a stable level.

Absolute quantification of SARS-CoV-2 DNA using digital CRISPR

We next characterized the assay performance of digital CRISPR in detecting and quantifying SARS-CoV-2 and compared it to that of digital PCR. In this assay, linearized plasmid containing the SARS-CoV-2 N gene was serially diluted and used as the target DNA in the aforementioned optimized digital CRISPR or digital PCR reactions. Using digital CRISPR-based detection, a proportional increase in the number of positive partitions was observed with increasing concentrations of the target DNA (Figure. 4A), indicating the good quantitative performance of digital CRISPR. Although few partitions in the negative control were classified as having a positive signal due to non-specific amplification, the average of 10 negative control replicates give us an average of 0.165 copies/µL readout and the limit of blank (LoB) is 0.413 copies/µL, which is about half of our limit of detection (LoD), 0.897 copies/µL (Figure 4A, Table S2).

To test the robustness and reproducibility of the digital CRISPR assay, at least ten independent digital CRISPR reactions using the SARS-CoV-2 N gene as the target DNA were performed on different days. The coefficient of variation (CV) observed for most samples was ≤15% except for the lowest dilution (0.6 copies/µL), indicating the limit of quantification (LoQ) of this method is around 2.2 copies/µL of the viral genome (Table S2). To assess the accuracy of digital CRISPR-based nucleic acid detection against that of digital PCR, DNA concentrations measured by digital CRISPR were plotted against the corresponding DNA concentrations obtained by digital PCR. Linear regression analysis revealed an R^2 value of above 0.99 across a dynamic range from 0.6 to 2027 copies/µL, suggesting that our digital CRISPR method was reliable for the absolute quantification of nucleic acids (Figure. 4B). These data highlight the sensitivity, accuracy, and speed of the digital CRISPR-based detection method developed in this study for the absolute quantification of nucleic acids in samples with LoD at 0.897 copies/µL and LoQ at 2.2 copies/µL.

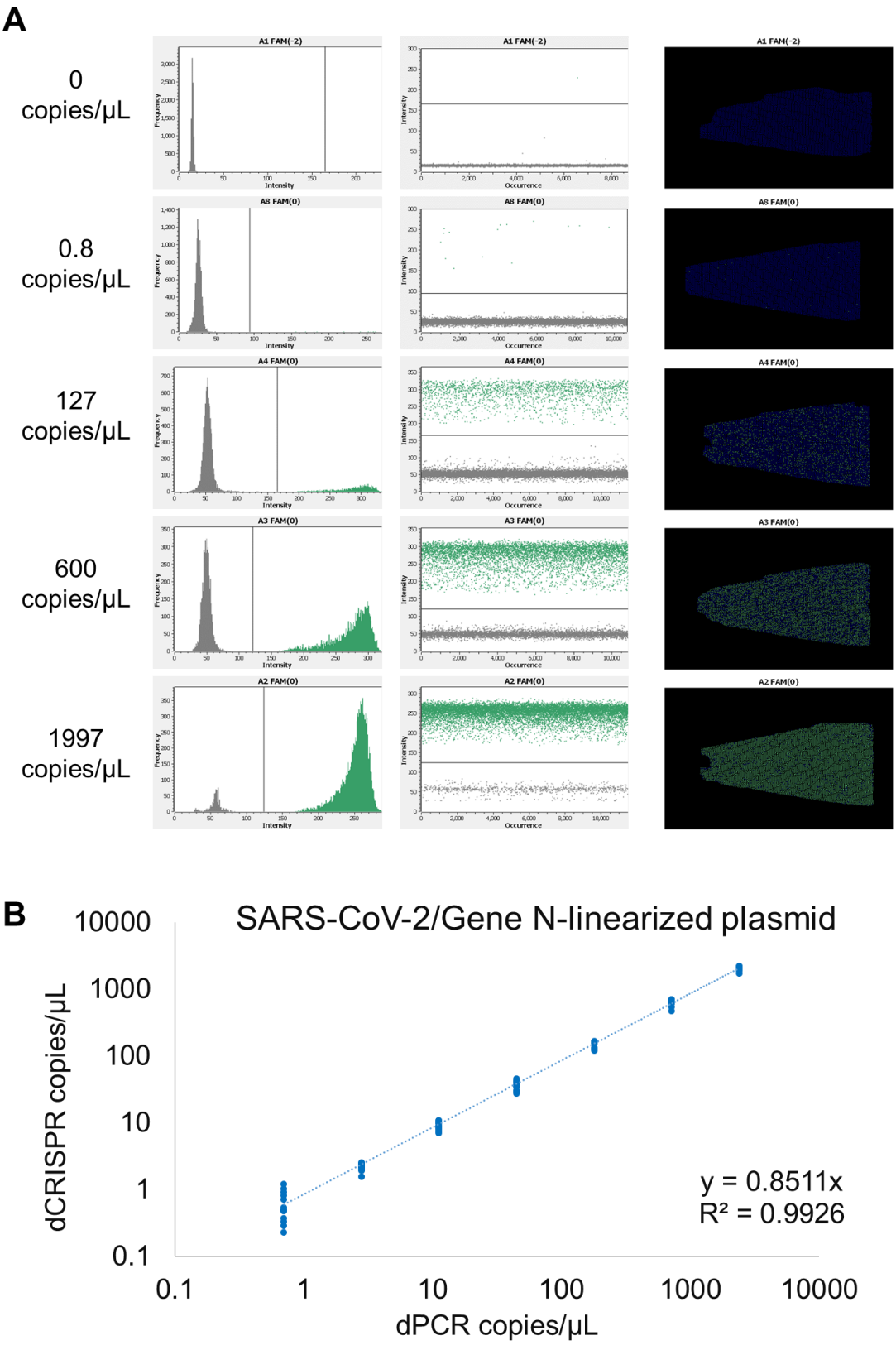

Figure 4. Digital CRISPR-based detection of different concentrations of SARS-CoV-2 N gene DNA. A. Fluorescence intensity histogram, scatter plot, and position plot of the partitions on the chip for serial dilutions of DNA. Four dilutions of linearized plasmid DNA encoding the SARS-CoV-2 N gene (0.8,

127, 600, 1997 copies/µL) and one non-template control (without plasmid DNA) were used as input DNA. The x-axis represents fluorescence intensity while the y-axis represents the frequency of the partitions. The left peak (low fluorescence level; dark grey) on the fluorescence intensity histogram represents the negative partitions while the right peak (high fluorescence level; green) indicates the positive partitions. In the scatter plot and position plot, each dot represents one partition on the chip. Green dots represent positive partitions with a high fluorescence level while grey or blue dots correspond to negative partitions with a low fluorescence level. **B.** Comparison of the absolute quantification result of digital CRISPR and digital PCR. Each point represents one sample. The original linearized plasmid DNA concentration was measured by using Clarity™ digital PCR and diluted to different concentrations (x-axis). The diluted DNA was then measured by using the digital CRISPR (dCRISPR) method. The calculated dCRISPR DNA concentrations are plotted on the y-axis.

Accuracy analysis of digital CRISPR-based quantification on circular plasmid

Plasmids are routinely used as reference DNA or standards in many analytical DNA measurements. However, conformational changes in supercoiled DNA have been reported to have a profound effect on PCR-based quantification [36-38]. Unsuccessful single-molecule amplification of non-linearized plasmids was reported in a PCR-based study, which resulted in an underestimation for circular plasmid quantification on some dPCR machines [39, 40]. To test whether plasmid conformation also affects the accuracy of digital CRISPR, undigested plasmid containing the SARS-CoV-2 N gene was serially diluted and used for digital PCR or digital CRISPR reactions. Concentrations of non-linearized plasmids measured by digital PCR were about half of those detected for linearized plasmids (regression coefficients at 0.5261) (Figure 5D), which is in accordance with previous studies and indicates that the accuracy of digital PCR is influenced by plasmid conformation. Compared to digital PCR, digital CRISPR-based detection showed higher amplification efficiency of the supercoiled plasmid DNA, as evidenced by the higher positive compartments ratio detected (Figure 5A, B). Digital CRISPR-based concentrations of non-linearized plasmids were highly concordant with those of linearized plasmids (regression coefficients at 1.0673) (Figure 5C), suggesting that the accuracy of digital CRISPR is not affected by plasmid conformation.

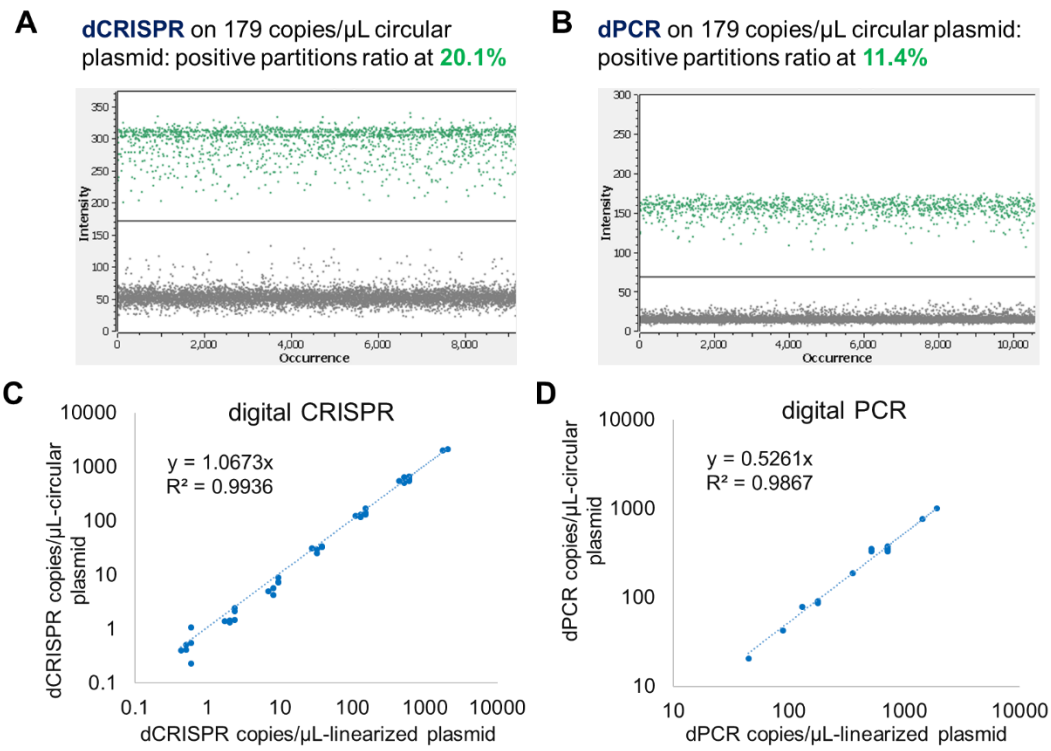

Figure 5. The effect of plasmid conformation on the accuracy of digital CRISPR (dCRISPR) and digital PCR (dPCR). A, B. The positive and negative partitions of dCRISPR (A) and dPCR (B) on detection of 179 copies/μL circular plasmid. **C, D.** Comparison of the absolute quantification result for linearized plasmid and circular plasmid of dCRISPR (C) and dPCR (D).

Specificity analysis of digital CRISPR-based detection

Primer and crRNA designs are key in determining the specificity of CRISPR-based nucleic acid detection assays. Previous studies have shown the ability of RPA to tolerate up to nine nucleotide base-pair mismatches across primer and probe binding sites [35]. To specifically detect SARS-CoV-2 using digital CRISPR, primers and crRNAs must be designed to specifically bind the SARS-CoV-2 target DNA and not its closely-related coronaviruses, such as MERS-CoV and other related human coronaviruses. We first analysed the binding sites of the primers and crRNAs that were originally designed based on the consensus sequence of the genome of 264 SARS-CoV-2 strains, available on the GISAID database [32, 41, 42]. The consensus sequence of these SARS-CoV-2 target regions was aligned with corresponding regions of SARS-CoV-2-related beta coronaviruses, such as SARS-CoV, MERS-CoV, and human coronaviruses Human-CoV 229E/HKU1/NL63/OC43. No cross-binding regions were observed with the other SARS-CoV-2-related coronavirus analyzed (Figure. S4A). A comparison between the binding site sequences of SARS-CoV-2 and its most similar relative, SARS-CoV, showed that there were 13 sequence variations across the primer and crRNA binding sites (three, two, and

seven sequence variations at the forward primer, reverse primer, and crRNA binding site, respectively). This is more than the nine nucleotide base-pair mismatch tolerance threshold for RPA, which therefore predicts the specificity of the designed primers and crRNA for SARS-CoV-2-specific CRISPR-based detection. To test the specificity of the reaction, we assayed the bulk RPA-Cas12a reaction using target plasmids containing the complete N gene from SARS-CoV-2, SARS-CoV, and MERS-CoV (Figure. S4B, C). Positive fluorescence signals were observed only in the reaction containing the SARS-CoV-2 plasmid, not in reactions containing SARS-CoV and MERS-CoV plasmids (Figure. S4B, C). The absence of cross-reactivity with the other related coronaviruses tested in this study validates the specificity of the CRISPR assay for SARS-CoV-2.

Background human DNA tolerance analysis of digital CRISPR-based detection

Previous studies have reported that RPA reactions could be inhibited by high concentrations of background human DNA [43, 44]. We therefore first tested the RPA-Cas12a bulk reaction in the presence of various concentrations of background human DNA (Figure. S5). In an RPA-Cas12a reaction with 37.5 copies/µL of target DNA, background human DNA concentrations below 2 ng/µL did not affect the reaction (Figure S5A). Concentrations of background human DNA above 5 ng/µL in a bulk RPA-Cas12a reaction showed reduced fluorescent signal intensities, which is in agreement with the inhibitory concentrations of background DNA reported in previous studies using bulk RPA reactions [44] (Figure. S5A).

We also tested for possible inhibitory effects of background DNA on reactions carried out in small partitions. In an RPA-Cas12a reaction with 400 copies/µL of target DNA, 1 ng/µL of background human DNA (equals to about 4350 human cells per reaction) did not affect the digital CRISPR reaction (Figure S5B). We also observed inhibition of the reaction containing 2 ng/µL of background human DNA, and complete inhibition of the reaction containing >5 ng/µL of background human DNA (Figure S5B). Nevertheless, since input DNA concentrations used for digital CRISPR-based detection are typically below 1 ng/µL, our findings suggest that background DNA will not inhibit the digital CRISPR reaction of samples within the dynamic range to be used for testing.

Previous studies have also reported that the tolerance of RPA for background DNA is dependent on target DNA concentrations present in the reaction [43, 44]. We therefore tested the effect of 1 ng/µL of background human DNA on digital CRISPR reactions with various concentrations of target DNA (Figure. S5C). Our results show that 1 ng/µL of background DNA did not affect reactions that contained target DNA concentrations within the dynamic range of digital PCR detection, i.e., 0.6 to 2027 copies/µL (Figure S5C). Our findings confirm that

the presence of background human DNA in the sample is not likely to affect the absolute quantification of the digital CRISPR reaction.

Digital CRISPR detection and absolute quantification of SARS-CoV-2 RNA

As SARS-CoV-2 is an RNA virus, we next tested whether digital CRISPR could be combined with reverse transcription (RT) in a one-pot reaction for the absolute quantification of RNA. RNA corresponding to the SARS-CoV-2 gene N target region was synthesized using a T7 promoter-tagged PCR product and T7 RNA polymerase, and different concentrations of RNA were tested in bulk RT-RPA-Cas12a reactions. Our results show a lower-than-expected sensitivity of the one-pot RT-RPA-Cas12a bulk reaction, with a detection limit at 244 copies/μL (Figure S6B). To assess if this decrease in sensitivity was in part due to an inefficient reverse transcription process in the one-pot reaction, we employed two reverse primers to facilitate the reverse transcription reaction and increase the sensitivity of the one-pot reaction. We detected an increase in sensitivity of 61 copies/μL when two reverse primers were used (Figure S6C).

We tested the sensitivity of the one-pot RT-RPA-Cas12a reaction in small partitions on digital CRISPR using varying concentrations of RNA. Notably, although the positive partition proportion increased with an increase in the concentration of input RNA, 1 copy of input RNA resulted in an increase of only 0.0177 copy as calculated by digital CRISPR, suggesting that the digital CRISPR method does not accurately quantify RNA (Figure S6D). Although the addition of two reverse primers increased the signal, it was insufficient to achieve a one-copy-per-partition sensitivity (Figure S6E). Our findings suggest that absolute quantification of RNA by digital CRISPR may require prior conversion to cDNA before the sample is analysed on a digital chip.

Absolute quantification of Epstein–Barr virus via digital CRISPR

Having demonstrated the accuracy of digital CRISPR on SARS-CoV-2 DNA samples, we tested the ability of our digital CRISPR method to perform absolute quantification of Epstein–Barr virus (EBV) DNA samples. To design primers and crRNA that were universal to both type Ⅰ and type Ⅱ EBV, the genomes of 16 EBV strains were analysed to identify conserved regions across all 16 EBV strains. A conserved DNA region within the Epstein-Barr nuclear antigen 1 (EBNA1) was used as the target sequence (Figure 6A). Viral DNA extracted from chemically-induced EBV-harboring human B cells was diluted to concentrations ranging from 0.5 to 2100 copies/μL, and used as the target DNA in both digital CRISPR and digital PCR reactions. In the digital CRISPR-based detection, samples loaded in the partition chip were incubated for 1 h at 42 °C, followed by endpoint fluorescence detection and copy number determination. Notably, the positive partition signal increased with an increase in the concentration of input EBV DNA (Figure 6B). The copy numbers measured by

digital CRISPR were in full agreement (R^2 value > 0.98) with those measured by digital PCR (Figure 6C). Our findings validate the accuracy and sensitivity of our digital CRISPR-based method for the absolute quantification of viral DNA rapidly within an hour, which is a 4-fold reduction in reaction time compared to digital PCR-based detection.

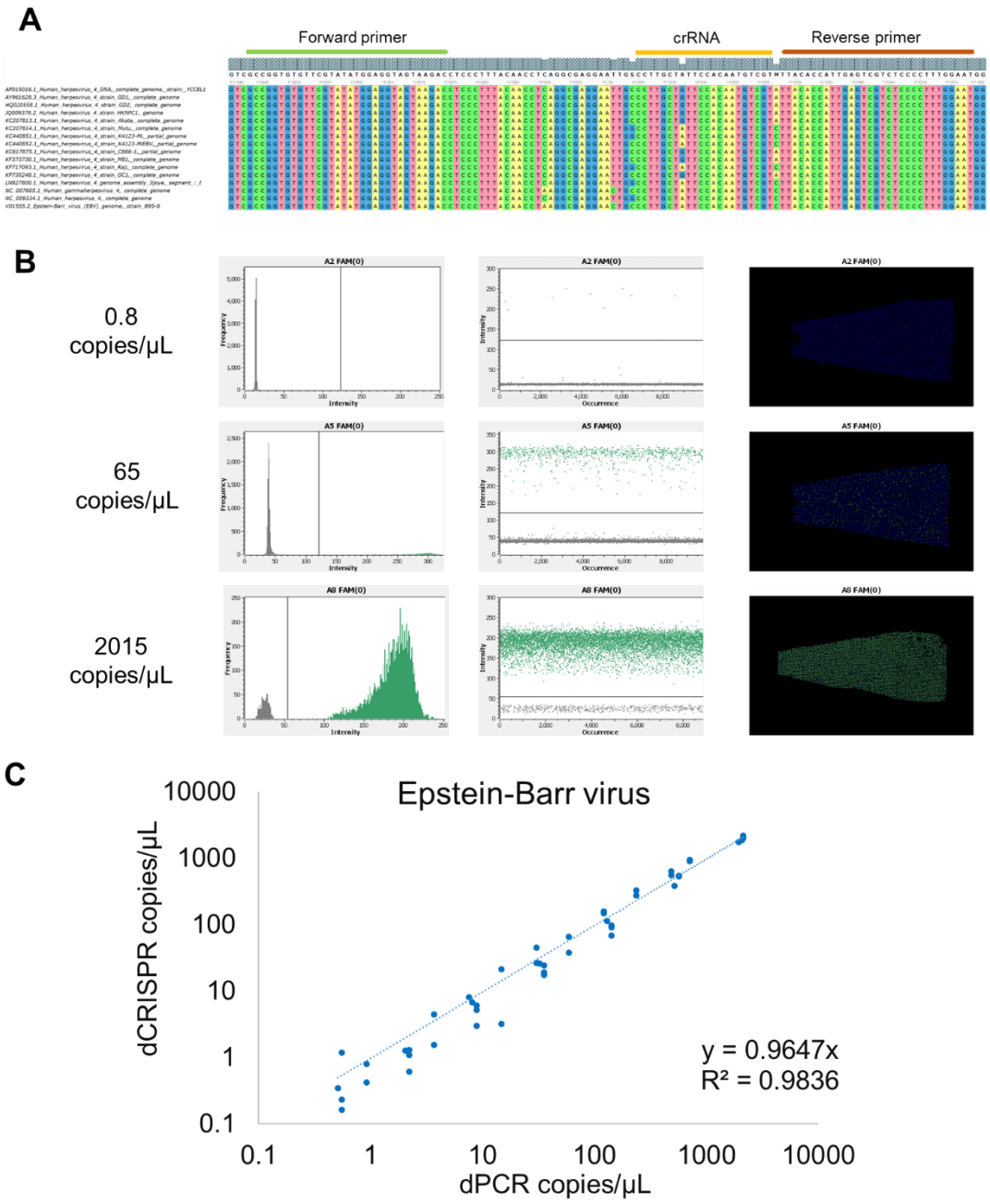

Figure 6. Absolute quantification of Epstein–Barr virus (EBV) by Digital CRISPR. A. Primer and crRNA design for digital CRISPR assay specific for EBV. **B.** Fluorescence intensity histogram, scatter plot, and position plot of the partitions on the chip on serially-diluted EBV DNA. **C.** A comparison of the absolute quantification values obtained from digital CRISPR and digital PCR methods using various concentrations of EBV DNA.

Discussion

In our study, we have developed a rapid and accurate digital CRISPR method for the absolute quantification of viral DNA. The performance characteristics of this method were validated using SARS-CoV-2 synthetic DNA and EBV DNA, and compared to those of absolute quantification digital PCR method, the current gold standard. Our digital CRISPR-based method achieved sensitivity and detection limits (LoD 0.897 copy/μL) comparable with those of qPCR and other isothermal methods, such as SHERLOCK and DETECTR (Table S3). The significant advantage of our digital CRISPR method over the other detection methods is its speed: our digital CRISPR method can perform absolute quantification rapidly within an hour, which is four times faster than current digital PCR-based detection.

Absolute quantification for viral detection could not only facilitate clinical processing but also benefit research. Viral loads closely parallel transmission risk and disease severity. High SARS-CoV-2 viral loads have been reported to correlate with the course of infection and mortality [7, 45-48]. These reports underscore the urgent need for rapid and sensitive virus detection and quantification methods to monitor viral load as the basis for clinical decision making. Such methods are also needed for mechanistic studies, transmission studies, vaccine development, and therapeutics for COVID-19. Although there currently exist many diagnostic methods available for virus detection, these methods usually do not allow for a rapid and precise quantification of the viral load (Table S3).

Our digital CRISPR-based method reported in the study is four times faster than the traditional digital PCR-based methods used for the absolute quantification of nucleic acids. Additionally, the isothermal feature of our digital CRISPR-based detection assay confers faster amplification of the viral target using a simple constant-temperature heat bath, enabling rapid viral detection that can be deployed even in low-resource areas. In recent years, other digital isothermal methods, such as RPA- or LAMP-based digital PCR methods, have been developed for detecting a variety of DNA targets [49-52]. However, these methods are limited by their low specificity, due to the inherent tolerance of RPA/LAMP-based methods for base-pair mismatches as compared to traditional PCR methods [53-58]. Our digital CRISPR method overcomes this by exploiting the specificity conferred by the Cas12a-crRNA-based targeting system. The collateral cleavage activity of Cas12a amplifies the signal and thus increases the sensitivity. Our digital CRISPR-based method combines the speed and sensitivity of isothermal amplification with the specificity of the CRISPR system.

Another advantage of our digital CRISPR method over other CRISPR-based methods [26-31] is its one-pot reaction design, which reduces manual manipulation

and increases reproducibility. In this streamlined one-pot reaction, both nucleic acid amplification and CRISPR-based detection are combined into a single step in a closed tube, significantly reducing the risk of cross-contamination between samples during batch processing. A major drawback of current CRISPR-based methods is the complexity of designing appropriate crRNAs that are limited to target regions in proximity to a PAM. This limitation may potentially complicate CRISPR-based virus detection since mutations in the viral PAM sequence may disable recognition by the Cas protein as the virus evolves. In contrast, our simpler digital CRISPR crRNA design is independent of the PAM sequence because it targets single-stranded DNA generated after amplification [34].

Our digital CRISPR method reported here uses commercially available chips and devices that can potentially be adapted to other devices already in use at some hospitals and service laboratories. These are QuantStudio 3D Digital PCR System (Thermo Fisher), QIAcuity Digital PCR System (QIAGEN), and Droplet Digital PCR System (Bio-Rad). We therefore envisage greater ease of adoption of our technology at these facilities. Furthermore, our digital CRISPR method offers a potentially customizable solution that is amenable to other DNA isothermal amplification platforms such as loop-mediated isothermal amplification, rolling circle amplification, and strand displacement amplification technologies, as well as the use of other Cas proteins, such as Cas13a, Cas12b, Cas14 for multiplex detection.

We have established and characterized a digital CRISPR method, which combines the speed and sensitivity of isothermal amplification, the specificity of CRISPR-based detection, and the ability to obtain absolute quantification by sample partitioning. Our digital CRISPR method detects a concentration of viral DNA as low as 0.897 copy/µL and enables rapid, absolute quantification with a dynamic range of 0.6 to 2027 copies/µL within one hour at a constant temperature, with no cross-reactivity to other similar viruses. Future work will focus on expanding the applications of our digital CRISPR method to areas such as gene expression analysis, rare mutant detection, copy number variation, and sequencing library quantification. Applications of such rapid analytics will also benefit cell therapy, pharmaceutical, environmental, public health, security and food industry to potentially determine the replication competency of adventitious agents.

Materials and methods

Materials

Preparation of primers and DNA targets: Oligonucleotides (primers), ssDNA-FQ reporters, SARS-CoV-2 N gene-containing G-Block, SARS-CoV-2, SARS-CoV, and MERS N gene-containing plasmids were synthesized by or purchased from Integrated DNA Technologies. The SARS-CoV-2 N gene-

containing plasmid was linearized using FastDigest ScaI (Thermo Scientific) and then used as DNA target. The SARS-CoV-2 N gene-containing plasmid was used as a template to amplify the N gene using primer N-RNA-F/ N-RNA-R by Platinum™ SuperFi II PCR Master Mix (Invitrogen). The PCR product was purified by QIAquick PCR Purification Kit (QIAGEN) and used as RNA synthesis template.

Synthetic RNA target preparation: Since N-RNA-F has a T7 promoter sequence, the amplified DNA using N-RNA-F/R primer will contain a T7 promoter upstream of gene N. The T7 tagged N gene dsDNA was transcribed into SARS-CoV-2 RNA using HiScribe™ T7 High Yield RNA Synthesis Kit (New England Biolabs) according to the manufacturer's protocol. The synthesized RNA was purified using Monarch® RNA Cleanup Kit (New England Biolabs) after treatment with DNase I (RNase-free, New England Biolabs).

crRNA preparation: Constructs were ordered as DNA from Integrated ssDNA Technologies with an appended T7 promoter sequence. crRNA ssDNA was annealed to a short T7 primer (T7-3G IVT primer [59] or T7-Cas12scaffold-F [60]) and treated with fill-in PCR (Platinum™ SuperFi II PCR Master Mix) to generate the DNA templates. These DNA were used as templates to synthesize crRNA using the HiScribe™ T7 High Yield RNA Synthesis Kit (New England Biolabs) according to published protocols [59, 60]. The synthesized crRNA was purified using Monarch® RNA Cleanup Kit (New England Biolabs) after treatment with DNase I (RNase-free, New England Biolabs), Thermolabile Exonuclease I (New England Biolabs), and T5 Exonuclease (New England Biolabs).

Primer and crRNA design

SARS-CoV-2 primers and crRNA were designed based on previously published papers [32] or 264 SARS-CoV-2 genome sequences from GISAID [41, 42]. Other human-related coronavirus sequences were downloaded from NCBI. UGENE software was used to analyze and align viral genomes (MUSCLE or Kalign). Consensus sequences (Threshold: 90%) of 264 SARS-CoV-2 genomes, 328 SARS-CoV, 572 MERS-CoV, 70 Human-CoV-229E genomes, 48 Human-CoV-HKU1 genomes, 71 Human-CoV-NL63, and 178 Human-CoV-OC43 were exported separately from UGENE and used for specificity analysis.

Epstein–Barr virus primers and crRNA were designed based on consensus sequences of 16 virus genomes including both type Ⅰ and type Ⅱ EBV (NCBI: AP015016.1, AY961628.3, HQ020558.1, JQ009376.2, KC207813.1, KC207814.1, KC440851.1, KC440852.1, KC617875.1, KF373730.1, KF717093.1, KP735248.1, LN827800.1, NC_007605.1, NC_009334.1, V01555.2).

Digital PCR quantification

SARS-CoV-2 N gene quantification: The G-block, plasmid, dsDNA and RNA concentrations were quantified by digital PCR. Serial dilutions of targets were mixed together with 500 nM CHNCDC-geneN-F, 500 nM CHNCDC-geneN-R, 250 nM CHNCDC-geneN-P, 1x TaqMan™ Fast Virus 1-Step Master Mix (for RNA, Applied Biosystems) or TaqMan™ Fast Advanced Master Mix (for DNA, Applied Biosystems), 1x Clarity™ JN solution (JN Medsys). For RNA samples, the reaction mixture was incubated at 55°C 10 min before partitioning the reaction mix on Clarity™ autoloader. Then the reaction partitions were sealed with the Clarity™ Sealing Enhancer and 230 µL Clarity™ Sealing Fluid, followed by thermal cycling using the following parameters: 95 °C for 15 min (one cycle), 95 °C 50 s and 56 °C 90 s (40 cycles, ramp rate = 1 °C/s), 70 °C 5 min. The endpoint fluorescence of the partitions was detected using Clarity™ Reader and the final DNA copy numbers were analyzed by Clarity™ software.

EBV quantification: Serial dilutions of EBV DNA was used for dPCR quantification by Clarity™ Epstein-Barr Virus Quantification Kit (JN Medsys) according to the manufacturer's protocol.

Cas12a bulk assay without preamplification

Unless otherwise indicated, 50 nM EnGen® Lba Cas12a (New England Biolabs), 50 nM crRNA, and 250 nM FQ ssDNA probe were incubated with dsDNA dilution series in NEB buffer 2.1 at 37°C, and fluorescence signals were measured every 5 min.

RPA-Cas12a bulk assay

The one-pot reaction combining RPA-DNA amplification and Cas12a detection was performed as follows: 300 nM forward primer, 300 nM reverse primer, 500 nM FQ probe, 1x RPA rehydration buffer containing 1 x RPA Pellet (TwistDx), 200 nM EnGen® Lba Cas12a (New England Biolabs), 200 nM crRNA, were prepared followed by adding various amounts of DNA input, and 14 mM magnesium acetate. When RNA was used as a target, 300 nM reverse primer 2 was used with 10 U/µL PhotoScript Reverse transcriptase (New England Biolabs) or 10 U/µL SuperScript™ IV Reverse Transcriptase (Invitrogen) and 0.5 U/µL RNase H (Invitrogen or New England Biolabs), as indicated. The reaction mixture was incubated at 42°C unless otherwise indicated and fluorescence kinetics were monitored every 1 min.

Digital CRISPR quantification

The digital CRISPR reaction was prepared by adding 1x Clarity™ JN solution (JN Medsys) to the RPA-Cas12a bulk reactions stated above. 15 µL of the mixture was loaded on the chip by a Clarity™ autoloader for sample partitioning. The reaction partitions were sealed with the Clarity™ Sealing Enhancer and

230 µL Clarity™ Sealing Fluid, followed by incubation at 42°C for 1 hour, unless otherwise indicated. After incubation, a Clarity™ Reader was used to read the fluorescent signal in the partitions, and Clarity™ software was used to calculate input DNA copy numbers.

Limit of Blank (LoB), Limit of Detection (LoD), and Limit of Quantitation (LoQ) calculation

LoB, LoD, and LoQ were calculated based on the following equation[61] using the statistics of digital CRISPR quantification on linearized plasmid in 10 replications (Table S2):

$LoB = \text{mean}_{blank} + 1.645 (SD_{blank})$

$LoD = LoB + 1.645 (SD_{\text{low concentration sample}})$

LoQ = the lowest concentration of CV ≤ 20%

Growing EBV-2 from Jijoye cells

Jijoye cells were treated with 4 mM sodium butyrate and 24 ng/ml tetradecanoyl phorbol acetate (TPA). Supernatants were harvested 4-5 days post-treatment by centrifugation at 4,000g for 20 min and passing over a 0.45 µm filter to remove cellular debris. Viral particles were pelleted by ultracentrifugation at 20,000 rpm for 90 min and resuspended in 1/100 the initial volume using complete RPMI or PBS if viruses were to be further purified. Concentrated viruses were further purified using OptiPrep gradient density ultracentrifugation at 20,000 rpm for 120 min, and the virus interface band collected and stored at -80°C for downstream analysis.

Epstein–Barr virus DNA extraction

EBV DNA was extracted using QIAamp DNA Mini Kit (QIAGEN) according to the manufacturer's protocol.

References

1. Wiersinga, W.J., Rhodes, A., Cheng, A.C., Peacock, S.J. & Prescott, H.C. Pathophysiology, Transmission, Diagnosis, and Treatment of Coronavirus Disease 2019 (COVID-19): A Review. *JAMA* (2020).
2. Sedlak, R.H. & Jerome, K.R. Viral diagnostics in the era of digital polymerase chain reaction. *Diagnostic microbiology and infectious disease* **75**, 1-4 (2013).
3. Lai, K.K., Cook, L., Wendt, S., Corey, L. & Jerome, K.R. Evaluation of real-time PCR versus PCR with liquid-phase hybridization for detection of enterovirus RNA in cerebrospinal fluid. *Journal of clinical microbiology* **41**, 3133-3141 (2003).

4. Boeckh, M. et al. Optimization of quantitative detection of cytomegalovirus DNA in plasma by real-time PCR. *Journal of clinical microbiology* **42**, 1142-1148 (2004).
5. Yao, X.-H. et al. Pathological evidence for residual SARS-CoV-2 in pulmonary tissues of a ready-for-discharge patient. *Cell research* **30**, 541-543 (2020).
6. Liu, Y. et al. Aerodynamic analysis of SARS-CoV-2 in two Wuhan hospitals. *Nature* **582**, 557-560 (2020).
7. Yu, F. et al. Quantitative Detection and Viral Load Analysis of SARS-CoV-2 in Infected Patients. *Clinical Infectious Diseases* (2020).
8. Kuypers, J. & Jerome, K.R. Applications of Digital PCR for Clinical Microbiology. *Journal of clinical microbiology* **55**, 1621-1628 (2017).
9. Salipante, S.J. & Jerome, K.R. Digital PCR—An Emerging Technology with Broad Applications in Microbiology. *Clinical chemistry* **66**, 117-123 (2020).
10. Whale, A.S. et al. Comparison of microfluidic digital PCR and conventional quantitative PCR for measuring copy number variation. *Nucleic acids research* **40**, e82-e82 (2012).
11. Dong, L. et al. Highly accurate and sensitive diagnostic detection of SARS-CoV-2 by digital PCR. *medRxiv*, 2020.2003.2014.20036129 (2020).
12. Martin, A. et al. High-sensitivity COVID-19 group testing by digital PCR. *arXiv preprint arXiv:2006.02908* (2020).
13. Lu, R. et al. SARS-CoV-2 detection using digital PCR for COVID-19 diagnosis, treatment monitoring and criteria for discharge. *medRxiv*, 2020.2003.2024.20042689 (2020).
14. Suo, T. et al. ddPCR: a more accurate tool for SARS-CoV-2 detection in low viral load specimens. *Emerg Microbes Infect* **9**, 1259-1268 (2020).
15. Liu, X. et al. Analytical comparisons of SARS-COV-2 detection by qRT-PCR and ddPCR with multiple primer/probe sets. *Emerging microbes & infections* **9**, 1175-1179 (2020).
16. Alteri, C. et al. Detection and quantification of SARS-CoV-2 by droplet digital PCR in real-time PCR negative nasopharyngeal swabs from suspected COVID-19 patients. *PloS one* **15**, e0236311 (2020).
17. Woloshin, S., Patel, N. & Kesselheim, A.S. False Negative Tests for SARS-CoV-2 Infection — Challenges and Implications. *New England Journal of Medicine* **383**, e38 (2020).
18. Notomi, T. et al. Loop-mediated isothermal amplification of DNA. *Nucleic acids research* **28**, E63-E63 (2000).
19. Tomita, N., Mori, Y., Kanda, H. & Notomi, T. Loop-mediated isothermal amplification (LAMP) of gene sequences and simple visual detection of products. *Nature protocols* **3**, 877-882 (2008).
20. Zhang, Y. et al. Rapid Molecular Detection of SARS-CoV-2 (COVID-19) Virus RNA Using Colorimetric LAMP. *medRxiv*, 2020.2002.2026.20028373 (2020).
21. Piepenburg, O., Williams, C.H., Stemple, D.L. & Armes, N.A. DNA Detection Using Recombination Proteins. *PLOS Biology* **4**, e204 (2006).
22. Daher, R.K., Stewart, G., Boissinot, M. & Bergeron, M.G. Recombinase Polymerase Amplification for Diagnostic Applications. *Clinical chemistry* **62**, 947-958 (2016).
23. Qian, J. et al. An enhanced isothermal amplification assay for viral detection. *bioRxiv*, 2020.2005.2028.118059 (2020).
24. Gootenberg, J.S. et al. Nucleic acid detection with CRISPR-Cas13a/C2c2. *Science* **356**, 438-442 (2017).
25. Chen, J.S. et al. CRISPR-Cas12a target binding unleashes indiscriminate single-stranded DNase activity. *Science* **360**, 436-439 (2018).
26. Gootenberg, J.S. et al. Multiplexed and portable nucleic acid detection platform with Cas13, Cas12a, and Csm6. *Science* **360**, 439-444 (2018).

27. Li, S.Y. et al. CRISPR-Cas12a-assisted nucleic acid detection. *Cell discovery* **4**, 20 (2018).
28. Myhrvold, C. et al. Field-deployable viral diagnostics using CRISPR-Cas13. *Science* **360**, 444-448 (2018).
29. Broughton, J.P. et al. CRISPR–Cas12-based detection of SARS-CoV-2. *Nature biotechnology* (2020).
30. Ackerman, C.M. et al. Massively multiplexed nucleic acid detection using Cas13. *Nature* (2020).
31. Hou, T. et al. Development and evaluation of a rapid CRISPR-based diagnostic for COVID-19. *PLOS Pathogens* **16**, e1008705 (2020).
32. Ding, X. et al. Ultrasensitive and visual detection of SARS-CoV-2 using all-in-one dual CRISPR-Cas12a assay. *Nature communications* **11**, 4711 (2020).
33. Low, H., Chan, S.-J., Soo, G.-H., Ling, B. & Tan, E.-L. Clarity™ digital PCR system: a novel platform for absolute quantification of nucleic acids. *Analytical and Bioanalytical Chemistry* **409**, 1869-1875 (2017).
34. Li, S.Y. et al. CRISPR-Cas12a has both cis- and trans-cleavage activities on single-stranded DNA. *Cell research* **28**, 491-493 (2018).
35. Li, J., Macdonald, J. & von Stetten, F. Review: a comprehensive summary of a decade development of the recombinase polymerase amplification. *The Analyst* **144**, 31-67 (2018).
36. Chen, J., Kadlubar, F.F. & Chen, J.Z. DNA supercoiling suppresses real-time PCR: a new approach to the quantification of mitochondrial DNA damage and repair. *Nucleic acids research* **35**, 1377-1388 (2007).
37. Hou, Y., Zhang, H., Miranda, L. & Lin, S. Serious Overestimation in Quantitative PCR by Circular (Supercoiled) Plasmid Standard: Microalgal pcna as the Model Gene. *PloS one* **5**, e9545 (2010).
38. Beinhauerova, M., Babak, V., Bertasi, B., Boniotti, M.B. & Kralik, P. Utilization of Digital PCR in Quantity Verification of Plasmid Standards Used in Quantitative PCR. *Frontiers in Molecular Biosciences* **7** (2020).
39. Dong, L., Meng, Y., Wang, J. & Liu, Y. Evaluation of droplet digital PCR for characterizing plasmid reference material used for quantifying ammonia oxidizers and denitrifiers. *Anal Bioanal Chem* **406**, 1701-1712 (2014).
40. Dong, L. et al. Comparison of four digital PCR platforms for accurate quantification of DNA copy number of a certified plasmid DNA reference material. *Scientific reports* **5**, 13174 (2015).
41. Elbe, S. & Buckland-Merrett, G. Data, disease and diplomacy: GISAID's innovative contribution to global health. *Global Challenges* **1**, 33-46 (2017).
42. Shu, Y. & McCauley, J. GISAID: Global initiative on sharing all influenza data – from vision to reality. *Eurosurveillance* **22**, 30494 (2017).
43. Clancy, E. et al. Development of a rapid recombinase polymerase amplification assay for the detection of Streptococcus pneumoniae in whole blood. *BMC infectious diseases* **15**, 481 (2015).
44. Rohrman, B. & Richards-Kortum, R. Inhibition of recombinase polymerase amplification by background DNA: a lateral flow-based method for enriching target DNA. *Analytical chemistry* **87**, 1963-1967 (2015).
45. Pujadas, E. et al. SARS-CoV-2 viral load predicts COVID-19 mortality. *The Lancet. Respiratory medicine* (2020).
46. Zheng, S. et al. Viral load dynamics and disease severity in patients infected with SARS-CoV-2 in Zhejiang province, China, January-March 2020: retrospective cohort study. *BMJ* **369**, m1443-m1443 (2020).
47. Zou, L. et al. SARS-CoV-2 Viral Load in Upper Respiratory Specimens of Infected Patients. *New England Journal of Medicine* **382**, 1177-1179 (2020).
48. Wölfel, R. et al. Virological assessment of hospitalized patients with COVID-2019. *Nature* **581**, 465-469 (2020).

49. Hu, F. et al. Smartphone-Based Droplet Digital LAMP Device with Rapid Nucleic Acid Isolation for Highly Sensitive Point-of-Care Detection. *Analytical chemistry* **92**, 2258-2265 (2020).
50. Lin, X., Huang, X., Urmann, K., Xie, X. & Hoffmann, M.R. Digital Loop-Mediated Isothermal Amplification on a Commercial Membrane. *ACS sensors* **4**, 242-249 (2019).
51. Ma, Y.D. et al. Digital quantification of DNA via isothermal amplification on a self-driven microfluidic chip featuring hydrophilic film-coated polydimethylsiloxane. *Biosensors & bioelectronics* **99**, 547-554 (2018).
52. Yeh, E.C. et al. Self-powered integrated microfluidic point-of-care low-cost enabling (SIMPLE) chip. *Sci Adv* **3**, e1501645 (2017).
53. Zhao, Y., Chen, F., Li, Q., Wang, L. & Fan, C. Isothermal Amplification of Nucleic Acids. *Chemical reviews* **115**, 12491-12545 (2015).
54. Lobato, I.M. & O'Sullivan, C.K. Recombinase polymerase amplification: Basics, applications and recent advances. *TrAC Trends in Analytical Chemistry* **98**, 19-35 (2018).
55. Mondal, D. et al. Mobile suitcase laboratory for rapid detection of Leishmania donovani using recombinase polymerase amplification assay. *Parasites & Vectors* **9**, 281 (2016).
56. Daher, R.K., Stewart, G., Boissinot, M., Boudreau, D.K. & Bergeron, M.G. Influence of sequence mismatches on the specificity of recombinase polymerase amplification technology. *Mol Cell Probes* **29**, 116-121 (2015).
57. Rolando, J.C., Jue, E., Schoepp, N.G. & Ismagilov, R.F. Real-Time, Digital LAMP with Commercial Microfluidic Chips Reveals the Interplay of Efficiency, Speed, and Background Amplification as a Function of Reaction Temperature and Time. *Analytical chemistry* **91**, 1034-1042 (2019).
58. Hardinge, P. & Murray, J.A.H. Reduced False Positives and Improved Reporting of Loop-Mediated Isothermal Amplification using Quenched Fluorescent Primers. *Scientific reports* **9**, 7400 (2019).
59. Kellner, M.J., Koob, J.G., Gootenberg, J.S., Abudayyeh, O.O. & Zhang, F. SHERLOCK: nucleic acid detection with CRISPR nucleases. *Nature protocols* **14**, 2986-3012 (2019).
60. Lucia, C., Federico, P.-B. & Alejandra, G.C. An ultrasensitive, rapid, and portable coronavirus SARS-CoV-2 sequence detection method based on CRISPR-Cas12. *bioRxiv*, 2020.2002.2029.971127 (2020).
61. Armbruster, D.A. & Pry, T. Limit of blank, limit of detection and limit of quantitation. *The Clinical biochemist. Reviews* **29 Suppl 1**, S49-52 (2008).

Acknowledgments

We thank Karen Pepper (MIT) and Scott A. Rice(NTU) for careful editing and helpful comments on the manuscript. This research is supported by the National Research Foundation, Prime Minister's Office, Singapore under its Campus for Research Excellence and Technological Enterprise (CREATE) programme, through Singapore MIT Alliance for Research and Technology (SMART): Critical Analytics for Manufacturing Personalised-Medicine (CAMP) Inter-Disciplinary Research Group.

Author Contributions

X.W., T.K.L., and H.Y. designed the research. X.W. developed the digital CRISPR based method, performed the experiment, and analyzed the data. C.C performed the Epstein–Barr virus culture and DNA extraction. Y.H.L., S.S., T.K.L., and H.Y. provided mentorship and feedback. X.W. wrote the original draft and all authors reviewed and edited the manuscript.

Competing Interests statement

X.W., T.K.L., and H.Y. are co-inventors on patent filings related to the published work. T.K.L. is a co-founder of Senti Biosciences, Synlogic, Engine Biosciences, Tango Therapeutics, Corvium, BiomX, Eligo Biosciences, Bota.Bio, and Avendesora. T.K.L. also holds financial interests in nest.bio, Ampliphi, IndieBio, MedicusTek, Quark Biosciences, Personal602Genomics, Thryve, Lexent Bio, MitoLab, Vulcan, Serotiny, and Avendesora.

Items included in Supplementary Materials：

Figures. S1 to S6

Tables S1 to S3

References